HAL open science

Microwave-dressed state-selective potentials for atom interferometry

V Guarrera, R Szmuk, J Reichel, P Rosenbusch

▶ **To cite this version:**

V Guarrera, R Szmuk, J Reichel, P Rosenbusch. Microwave-dressed state-selective potentials for atom interferometry. New Journal of Physics, 2015, 17 (8), pp.083022. 10.1088/1367-2630/17/8/083022 . hal-01188057

HAL Id: hal-01188057

https://hal.sorbonne-universite.fr/hal-01188057v1

Submitted on 31 Aug 2015

HAL is a multi-disciplinary open access archive for the deposit and dissemination of scientific research documents, whether they are published or not. The documents may come from teaching and research institutions in France or abroad, or from public or private research centers.

L'archive ouverte pluridisciplinaire **HAL**, est destinée au dépôt et à la diffusion de documents scientifiques de niveau recherche, publiés ou non, émanant des établissements d'enseignement et de recherche français ou étrangers, des laboratoires publics ou privés.

Distributed under a Creative Commons Attribution 4.0 International License

IOPscience iopscience.iop.org

Home Search Collections Journals About Contact us My IOPscience

Microwave-dressed state-selective potentials for atom interferometry

This content has been downloaded from IOPscience. Please scroll down to see the full text.

2015 New J. Phys. 17 083022

(http://iopscience.iop.org/1367-2630/17/8/083022)

View the table of contents for this issue, or go to the journal homepage for more

Download details:

IP Address: 134.157.80.70
This content was downloaded on 27/08/2015 at 15:22

Please note that terms and conditions apply.

New Journal of Physics
The open access journal at the forefront of physics

Deutsche Physikalische Gesellschaft DPG
IOP Institute of Physics

Published in partnership with: Deutsche Physikalische Gesellschaft and the Institute of Physics

CrossMark

OPEN ACCESS

RECEIVED
20 February 2015

REVISED
22 May 2015

ACCEPTED FOR PUBLICATION
25 June 2015

PUBLISHED
11 August 2015

Content from this work may be used under the terms of the Creative Commons Attribution 3.0 licence.

Any further distribution of this work must maintain attribution to the author(s) and the title of the work, journal citation and DOI.

PAPER

Microwave-dressed state-selective potentials for atom interferometry

V Guarrera[1], **R Szmuk**[1], **J Reichel**[2] **and P Rosenbusch**[1]

[1] LNE-SYRTE, Observatoire de Paris, PSL Research University, CNRS, Sorbonne Universités, UPMC University Paris 06, 61 Avenue de l'Observatoire, 75014 Paris, France

[2] Laboratoire Kastler Brossel, ENS, UPMC-Paris 6, CNRS, College de France, 24 rue Lhomond, F-75005 Paris, France

E-mail: vera.guarrera@obspm.fr **and** peter.rosenbusch@obspm.fr

Keywords: atom interferometry, Bose–Einstein condensates, atom chip

Abstract

We propose a novel and robust technique to realize a beam splitter for trapped Bose–Einstein condensates (BECs). The scheme relies on the possibility of producing different potentials simultaneously for two internal atomic states. The atoms are coherently transferred, via a Rabi coupling between the two long-lived internal states, from a single well potential to a double-well. We present numerical simulations supporting our proposal and confirming excellent efficiency and fidelity of the transfer process with realistic numbers for a BEC of ^{87}Rb. We discuss the experimental implementation by suggesting state-selective microwave (MW) potentials as an ideal tool to be exploited for magnetically trapped atoms. The working principles of this technique are tested on our atom chip device which features an integrated coplanar MW guide. In particular, the first realization of a double-well potential by using a MW dressing field is reported. Experimental results are presented together with numerical simulations, showing good agreement. Simultaneous and independent control on the external potentials is also demonstrated in the two Rubidium clock states. The transfer between the two states, featuring respectively a single and a double-well, is characterized and it is used to measure the energy spectrum of the atoms in the double-well. Our results show that the spatial overlap between the two states is crucial to ensure the functioning of the beamsplitter. Even though this condition could not be achieved in our current setup, the proposed technique can be realized with current state-of-the-art devices being particularly well suited for atom chip experiments. We anticipate applications in quantum enhanced interferometry.

1. Introduction

In recent years, Bose–Einstein condensates (BECs) have proven to be appealing systems for the realization of atom interferometers, owing to their properties of macroscopic phase coherence [1]. Furthermore the possibility to interact with the environment, including electro-magnetic radiation, and their inertial nature promote them as powerful sensors. Interparticle interactions are also a fundamental ingredient as they are responsible for multi-particle entanglement which is known to lead to a phase estimation uncertainty below the standard shot-noise limit. Recently, a few experiments with BECs have initiated this path by exploiting spin squeezing [2–4]. Even though they are not yet better performing than the best state-of-the-art atom interferometers, which are mainly limited by shot-noise (the standard quantum limit), BEC based in-trap interferometers will be crucial for local probing on the scale of few microns, due to their small size, and for application requiring a relatively low atom number. Possible usages include compact electro-magnetic and inertial forces sensing devices. State-of-the-art BECs interferometers suffer from technical noise as finite temperature effects, excitations, detection noise as well as phase diffusion in configurations working with trapped atomic ensembles [5] which limit the phase sensitivity above the standard quantum limit. Reducing technical noise in the process of beam splitting and read out as well as elaborating new strategies that can lead to

© 2015 IOP Publishing Ltd and Deutsche Physikalische Gesellschaft

reach and also beat the shot-noise limit are nowadays crucial topics. In particular, commonly employed techniques to split the atomic cloud in a trap can cause excitations limiting the coherence time [6, 7] and involve dynamics affecting the initial phase coherence between the two separated clouds in a non-trivial way [8]. Much effort has been dedicated through the years to optimize these same techniques while novel ones, capable of definitely solving these problems, have not been found yet.

To accomplish this task, we propose here a novel scheme for a robust and fast beam splitter with trapped BECs which does not require a dynamical variation of the trapping potential, neither a momentum transfer to the atoms. The atoms are initially prepared in an internal state $|1\rangle$ in a single well potential. At the same time a double-well potential is generated selectively for a second internal state $|2\rangle$. The splitting is realized by transferring the atoms from state $|1\rangle$ to state $|2\rangle$ by means of a π-pulse of coherent electromagnetic radiation. We perform numerical simulations of this scheme, demonstrating nearly unitary efficiency in the transfer to the ground state of the double-well potential. As it concerns the experimental implementation, this requires the realization of external potentials which are different for the two internal states, $|1\rangle$ and $|2\rangle$, and to create a double-well for the state $|2\rangle$. Few techniques exist to drive state-dependent potentials: radio-frequency dressing or microwave (MW) dressing of magnetically trapped states and dipole forces by optical beams with proper wavelength and polarization. The solution which we consider here implies the use of state-selective MW-dressed potentials. We report experimental results showing that the proposed splitter can be notably realized on a compact atom chip device, by a MW near-field.

This paper is organized as follows: in section 2 we discuss the proposed scheme in a detailed way, analysing its features and constraints. We present numerical simulations based on coupled Gross–Pitaevskii equations, demonstrating the feasibility of the proposal under realistic experimental conditions. We consider, in particular, BECs of ^{87}Rb in their two hyperfine ground states. In section 3 we investigate the use of MW dressing to shape the underlying magnetic trap and to obtain independently controlled external potentials for the two different internal states. We exploit our atom chip device to experimentally prove the working principles of this strategy. We report, in particular, on the first realization and characterization of a MW-dressed double-well potential. In section 4 we finally prove independent and simultaneous control over the external potentials for the two hyperfine states $|F = 1,\ m_F = -1\rangle$ and $|F = 2,\ m_F = 1\rangle$ of ^{87}Rb on our atom chip. We characterize the atom transfer between these two levels and we demonstrate the importance of independently dressing the two states in order to adjust the spatial overlap of the clouds to optimize the process. A measurement of the atomic energy spectrum in the double well potential can be derived for different intensities of the dressing field. Finally we discuss further experimental developments by means of state-of-the-art devices and possible applications of the presented technique.

2. A beam splitter based on state-selective potentials

A common way to split a BEC for interferometric purposes consists of dynamically raising a potential barrier in the centre of the atomic distribution. The potential in which the atoms sit thus gradually evolves from a harmonic one to a double-well. For a given barrier height, the properties of the final state strongly depend on the duration of the splitting ramp and on the interatomic interactions [9–11]. Long ramping-up times are generally required to reduce unwanted excitations, making the process as adiabatic as possible. Note that during the ramping-up the energy of the first excited state progressively approaches the one of the ground state to the point of becoming degenerate. An ideally adiabatic transfer cannot thus be reached even for long times, i.e. longer than the typical BEC lifetimes of standard experiments [10], and excitations are produced. As a consequence subsequent manipulations and interrogation of the atomic systems should be performed faster than the timescales of the detrimental processes initialized during the splitting. On the other hand, the preservation of the phase coherence between the two separated clouds imposes some stringent limitation on the maximum duration of the ramping-up dynamics [11]. In order to avoid both to excite the cloud and to compromise its phase coherence, here we propose a novel, robust beam-splitter in which the double-well potential is not gradually raised up but the atoms are instead transferred from a single-well potential to a double-well by a π-like pulse between two different long-lived internal states $|1\rangle$ and $|2\rangle$, as depicted in figure 1. This procedure allows the atoms to reach their final split state $|2\rangle$ without passing through a deformation of the trapping potential itself, thus avoiding intrinsic excitations.

By using coherent electro-magnetic pulses to transfer the atoms to the double-well potential, we can address the exact final vibrational states which we want to populate, e.g. the ground state as required in this proposal, by properly tuning the frequency of the pulse. To perform a transfer to single eigenstates of the double-well potential, one additionally requires the duration of the pulse τ to be sufficiently long with respect to the timescales set by the confining potentials $\tau \sim \pi/\Omega \gg 1/\omega_{ho}$, where Ω is the frequency of the Rabi coupling and ω_{ho} is the trapping frequency along the splitting direction.

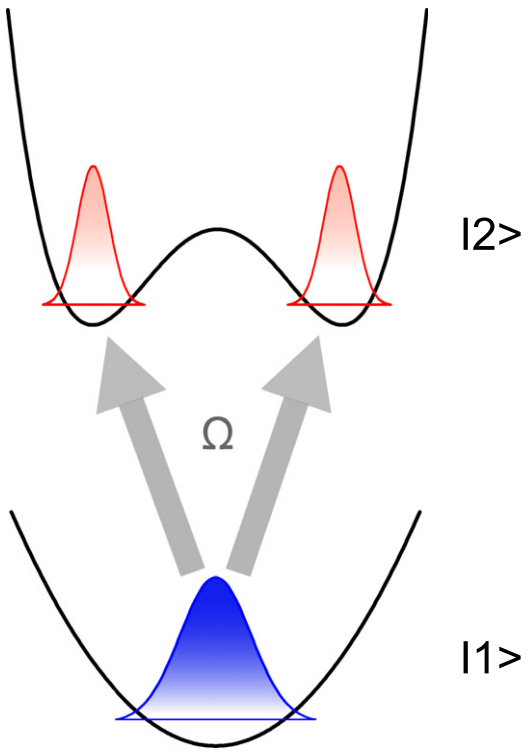

Figure 1. Schematics of the beam-splitter: atoms are transferred from a single to a double-well by coherently coupling (with Rabi frequency Ω) two long-lived internal states in the presence of a state-selective potential.

The phase coherence between the separated clouds in the internal state $|2\rangle$ does not depend on the details of the dynamics that they follow during the splitting but is ideally set by the Rabi coupling which phase-locks each of them to the atomic cloud in the other internal state $|1\rangle$. This guarantees the final split state to be prepared in a coherent superposition of two spatial modes which are localized at each well of a double-well potential in absence of significant direct inter-site tunnelling. This technique can be of great benefit for atom interferometry: the phase coherence between the spatial modes is preserved while the coherent coupling to the state $|1\rangle$ is active and is ideally decoupled from the dynamics of the splitting cloud. Moreover, realizing an ideal coherent state in a separated double-well potential would give the possibility to observe interaction induced squeezing, over-squeezing and the formation of phase cat states [12, 13].

Depending on the ratio Λ between the effective interaction energy and the Rabi frequency, different regimes are expected [14], in the approximation of identical spatial modes of the coupled states. In particular, for $\Lambda < 1$ in the so-called Rabi regime the linear coupling is governing the time evolution and single-particle coherence is preserved [15]. For $\Lambda > 1$ interactions start to play an important role, the Josephson regime is entered and for $\Lambda > 2$ self-trapping modes (also with running-phase) appear. Atom transfer within internal states is progressively inhibited and also single-particle coherence is gradually lost [15]. An ideal coherent atom transfer would thus require $\Lambda \lesssim 2$. As $\Omega \ll \omega_{ho}/\pi$ to guarantee the absence of unwanted excitations during the process, the above condition is fulfilled only for small enough interaction energies. These are achievable in current experiments, for example, with the use of Feshbach resonances [14]. Another possibility consists of dynamically varying the detuning of the Rabi pulse $\delta(t)$ in order to compensate for the effects of the interparticle interactions, as we will show.

In the case we consider in this paper, the two spatial modes of the states $|1\rangle$ and $|2\rangle$ are different and their wavefunction overlap plays an important role in the transfer dynamics, see figure 2. This is responsible for the vibrational states that the atoms preferably occupy once they are transferred, for a given detuning of the pulse. It also strongly affects the effective time of the transfer and the overall fraction of atoms that can be moved to state $|2\rangle$, when dealing with interacting particles. In a simple single-atom picture, the amplitude of the transfer probability to the nth-vibrational state of the double-well potential $|2,\ n\rangle$ can be written as $P_n = \frac{C_n\Omega}{\sqrt{(C_n\Omega)^2 + \Delta_n^2}}$ where $C_n = |\langle 2,\ n|1\rangle|$ is the wavefunction overlap of the nth-state with the initial state $|1\rangle$ and Δ_n the pulse detuning to the nth-state, see also [16]. Thus, in order to mainly occupy the ground state (n= 0), one requires $C_n \ll \Delta_n/\Omega$ for $n = 1,\ 2,\ 3$ ... This imposes a condition on the trap frequencies in $|1\rangle$, on the barrier height and

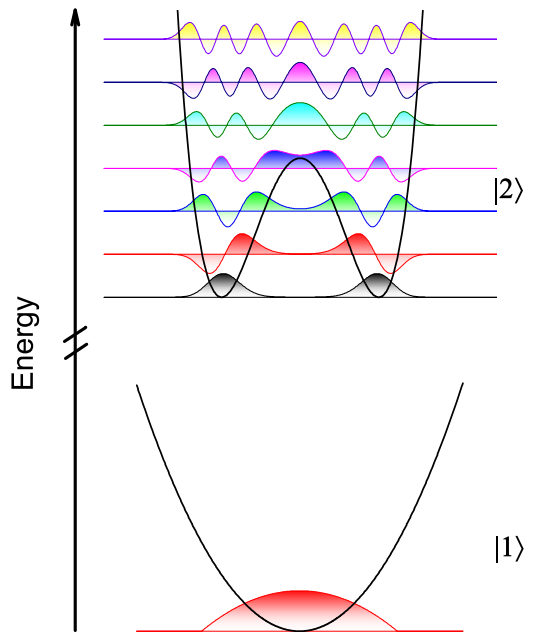

Figure 2. Real part of the symmetric wavefunctions for a BEC in the single trap and for different vibrational states in the double well. It appears clear that a better spatial overlap of the two external potentials in $|1\rangle$ and $|2\rangle$ would lead to a better matching of the initial BEC with the low lying energy states in the double-well. Higher energy separation between the eigenstates, E_n, and lower values of Ω reduce the contribution of the higher excited states in the transfer dynamics. The wavefunctions shown here refer to the set of parameters used in section 2.1.

separation of the minima of the double-well potential in $|2\rangle$, and on the Rabi frequency. In particular one configuration appears preferably suited for our proposal: the overlap with the ground state $|1\rangle$ is higher for the lower lying energy states in $|2\rangle$, i.e. $d/(2R) \lesssim 1$ with d the minima separation in the double well and R the Thomas–Fermi radius of the BEC in $|1\rangle$, and $\Delta_n/\Omega \gg 1$ to guarantee the occupation of the ground state with high fidelity. In the case where the overlap is higher for the higher lying energy states in the double-well, $d/(2R) \gg 1$, and Δ_n/Ω is large enough, occupation of the sole ground state can still take place but at the price of long transfer times, according to the low values of C_0.

The absolute value of $\tau \sim \pi/\Omega$ should indeed be safely smaller than typical timescales of irreversible dephasing due to technical and intrinsic reasons, including instabilities of the magnetic fields and finite lifetime of the atomic samples in the traps. From previous experimental observations, we can estimate this limit for ^{87}Rb atoms with typical trapping configurations to be given by the shortest lifetime in the usual clock states, which is ~100 ms.

2.1. Numerical simulations

In order to more precisely characterize and to test our method, we numerically model the dynamics of two wave functions ψ_1 and ψ_2 with two coupled 1D Gross–Pitaevskii equations including the linear coupling due to the field driving Rabi oscillations:

$$\begin{aligned} i\hbar\frac{\partial}{\partial t}\psi_1 &= \left[-\frac{\hbar^2\nabla^2}{2\,m} + V_1 + g_{11}\,|\psi_1|^2 + g_{12}|\psi_2|^2 - \frac{\delta}{2}\right]\psi_1 - \frac{\hbar\Omega}{2}\psi_2 \\ i\hbar\frac{\partial}{\partial t}\psi_2 &= \left[-\frac{\hbar^2\nabla^2}{2\,m} + V_2 + g_{22}\,|\psi_2|^2 + g_{21}|\psi_1|^2 + \frac{\delta}{2}\right]\psi_2 - \frac{\hbar\Omega}{2}\psi_1, \end{aligned} \tag{1}$$

where m is the mass of the atom and δ the detuning with respect to the considered atomic transition [17]. The effective one-dimensional interaction parameters are $g_{ij} = \frac{4\pi\hbar^2 a_{ij}}{m}\frac{1}{a_\perp^2}$ with a_{ij} the intra-state ($i=j$) and inter-state ($i \neq j$) scattering lengths and $a_\perp$ the average harmonic oscillator length in the radial direction of the trap. Numerical calculations are performed by means of the time-splitting spectral method developed in [18]. In figure 3 we show results for a BEC with $N = 500$ atoms of ^{87}Rb, where the internal states $|1\rangle$ and $|2\rangle$ correspond respectively to the hyperfine ground states $F = 1$ and $F = 2$. The initial trap $V_1(x)$ is harmonic with frequency $2\pi \times 500$ Hz and the double-well potential is approximated by the simple expression $V_2(x) = \frac{V}{(d/2)^4}(x^2 - (d/2)^2)^2$ with barrier height $V/\mu_2 = 6.6$, where μ_2 is the chemical potential in the double-well. The final trapping frequency is $\omega \simeq 2\pi \times 2100$ Hz. The distance between the two potential minima is

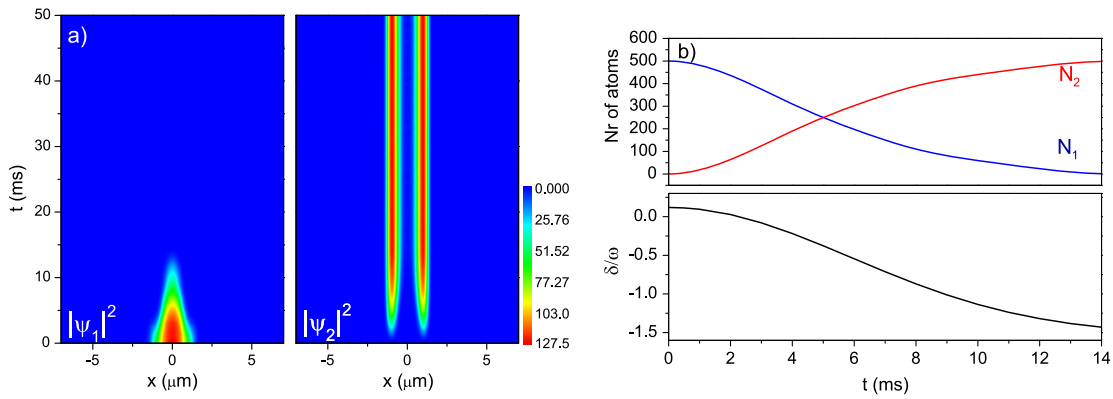

Figure 3. (a) Density distribution of the atoms in $F = 1$ (left) and $F = 2$ (right) as a function of time. A Rabi coupling between the two states is applied for 14 ms. (b) In the upper panel the atom number N_1 and N_2 in the two states is shown as a function of time. The frequency of the pulse is numerically optimized to maximize the efficiency of the transfer, in the lower panel the resulting detuning $\delta(t)$ is reported in units of the final trapping frequency.

taken to be $d = 2\,\mu$m. The frequencies in the radial direction are $2\pi \times (50,\ 500)$ Hz, setting $d/(2R) = 0.9$. We transfer the atoms from the $F = 1$ to the $F = 2$ ground state in 14 ms with a pulse of Rabi frequency $\Omega = 2\pi \times 100$ Hz ($\Lambda \sim 1.9$). A compensation of the energy shift due to interactions is accomplished by varying δ to maximize the number of atoms transferred at each computational time step. In this way, by dynamically varying the detuning as shown in figure 3, we can transfer 100% of the atoms to the internal state $F = 2$. The chirping of the transfer pulse compensates also for the change in the interspecies mean-field energy described by the third terms on the right-hand side of both equations (1). In particular, as can be seen in figure 3(a), for small t the mean field potential exerted by the atoms in $|1\rangle$ produces a small shift of the centers of the wells for the atoms in $|2\rangle$. As the atoms are progressively transferred this potential terms gradually vanishes and the final potential coincides with V_2. In order to characterize the fidelity of the wavefunction transfer [19], we calculate $f = \int \mathrm{d}x\,|\psi_2^*(x,\ t)|\cdot|\psi_{2,gs}(x,\ t)|$, where $\psi_{2,gs}(x,\ t)$ corresponds to the final ground state in $F = 2$, calculated for the same atom number. For the case presented above the fidelity oscillates between $f = 0.99994$ and $f = 0.99998$, after the transfer has been completed. We have additionally verified that our technique is robust against noise fluctuations that are usually present in real experiments and that could lead to small asymmetries between the two wells. Even for fluctuations of the zero-point energies of the two wells of $0.2 \times \hbar\omega$ we have obtained 100% transfer efficiency and fidelities that oscillate between 0.9996 and $f = 0.99995$. The system, which we have numerically studied, is an emblematic realization, with realistic experimental parameters, of the beam splitter which we propose in the present paper. Provided that the wavefunction overlap between the two coupled states is good, and that the ratio between the energy spacing of the low-lying eigenstates of the double well and the Rabi frequency is large enough, we have demonstrated that the ground state of the double well can be populated with excellent efficiency and fidelity. As a result no unwanted excitation have occurred during the transfer and the final state is ideally phase coherent.

3. Experimental realization of MW-dressed potentials

The realization of our proposal requires the BEC sample to be transferred from a single-well potential to a double well, in a controlled way by a coherent pulse. Experimentally this is far from being a trivial task: the atoms should hence experience two different potentials (single and double-well), acting simultaneously on two different long-lived internal states which can be conveniently coupled by electro-magnetic radiation. The solution we adopt consists in coherently manipulating the BEC with state dependent MW potentials. This technique has been employed before to selectively control the density distribution of ^{87}Rb atoms in the clock states $|F = 1,\ m_F = -1\rangle$ and $|F = 2,\ m_F = 1\rangle$ [20, 21]. The oscillating MW field $\mathbf{B}_{\mathrm{mw}}(\mathbf{r})$ couples the different hyperfine states of the ground state via magnetic dipole transitions, see figure 4 for a scheme of the relevant levels and transitions. As a result of the action of the MW field which is continuously shone on the atoms, each state is dressed, i.e. is shifted in energy by the amount $V_{\mathrm{mw}}(\mathbf{r})$, effectively an AC-Zeeman shift which has a spatial dependence. The MW induced potential can be approximated by

$$V_{\mathrm{mw}}(\mathbf{r}) \approx \sqrt{|\Omega_{1,m_1}^{2,m_2}|^2 + |\Delta_{1,m_1}^{2,m_2}|^2} - |\Delta_{1,m_1}^{2,m_2}|, \tag{2}$$

where: (i) the Rabi frequency $\Omega_{1,m_1}^{2,m_2}(\mathbf{r})$ depends on the projection of $\mathbf{B}_{\mathrm{mw}}(\mathbf{r})$ along the direction parallel (normal), for linear (circular) polarizations, to the quantization axis set by the static magnetic field $\mathbf{B}(\mathbf{r})$ and (ii)

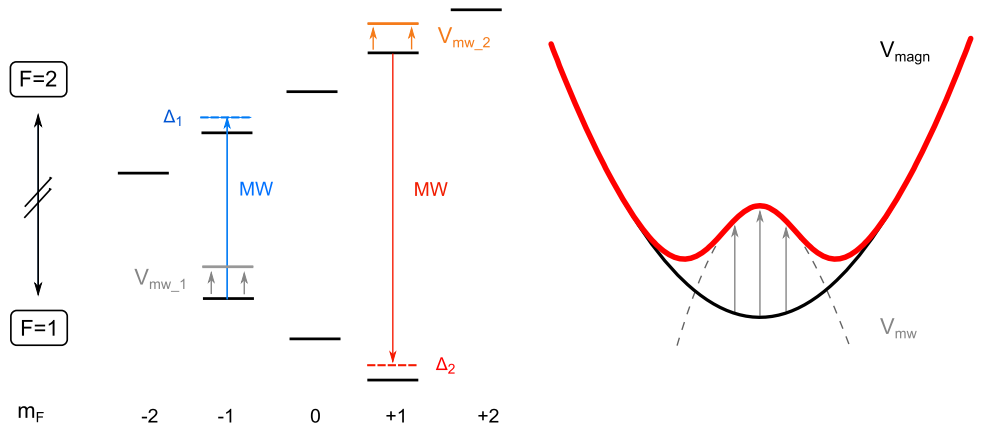

Figure 4. (Left) Level scheme of the ^{87}Rb ground state in presence of an external magnetic field. The dressing transitions which we use in the present work are also indicated. Due to the MW field the atomic levels are shifted in energy by the amount $V_{\mathrm{mw}}(\mathbf{r})$, effectively an AC-Zeeman shift with a spatial dependence. (Right) To create a double well potential a repulsive barrier V_{mw} is grown in the center of the magnetic trap V_{magn} along one of its axis. The overall potential $V = V_{\mathrm{magn}} + V_{\mathrm{mw}}$, depicted as a thick solid red line shows two symmetric local minima forming a double-well.

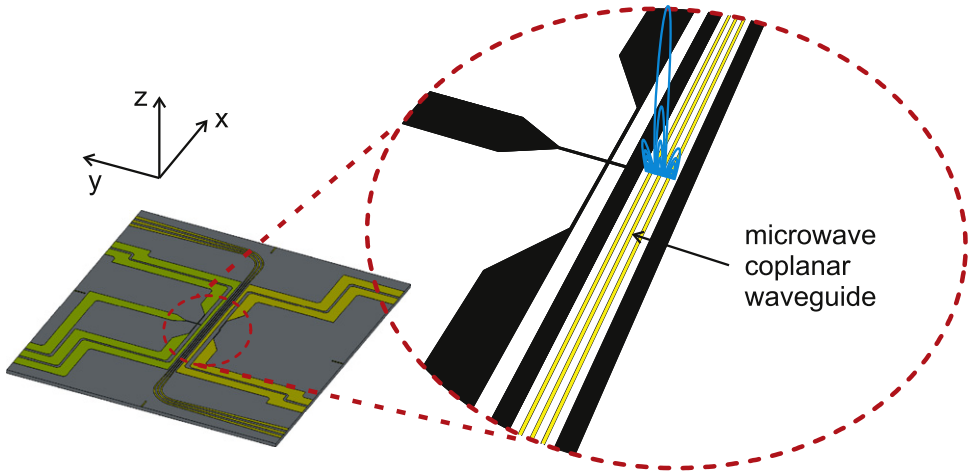

Figure 5. Schematics of the chip first layer. A zoom in the centre of the chip shows the three wires which form the microwave coplanar waveguide. The central wire of the CPW is used, in addition, to carry the stationary current for the generation of the magnetic trap. In the present realization the two side wires of the CPW are grounded at the chip.

the detuning $\Delta_{1,m_1}^{2,m_2}(\mathbf{r}) = (\omega - \omega_{hfs}) - (m_2 - m_1)\mu_B|\mathbf{B}(\mathbf{r})|$, with ω_{hfs} the frequency of the field free hyperfine transition. This energy shift is varying in space through its dependence on the spatial mode of the MW and on the static magnetic field and it can be used to reshape the underlying magnetic potential $V_{\mathrm{magn}}(\mathbf{r})$ used to trap the atoms, as shown in figure 4. Moreover, in presence of a large enough Zeeman splitting of the hyperfine states, the MW-coupling can be effective only for some sublevels, leaving the others mainly unperturbed. This feature can be used to create state-selective, independently tunable potentials. We note that MW dressed potentials present some advantages with respect to other state-selective techniques. Firstly, RF dressing techniques do not provide independent control on the different internal states and, secondly the use of optical potentials will suffer from spontaneous incoherent scattering by the trapping beams.

We experimentally implement the MW dressed potentials by using an atom chip device with an integrated coplanar waveguide (CPW) for exploitation of the MW near field. The design of the two-layer chip has been described in previous publications, see for example [22]. We only recall here that our CPW is made of three gold wires parallel to the x axis (see figure 5 for axis orientation) each of size $(L_y, L_z) = (50, 10)\,\mu$m and centres displaced by 150 μm along the y direction. The two side wires are grounded, whereas the central one is also used to carry the dc-current which sets one of the confining axis of the Ioffe–Pritchard trap $\mathbf{B}(\mathbf{r})$.

In our working configuration, which is depicted in figure 6(a), the elongated Ioffe trap is oriented with its weak axis orthogonal to the axis of the CPW, i.e. $\mathbf{B}_{\mathrm{Ioffe}} \| \mathbf{y}$. To realize a double well in one of the selected internal states, a repulsive potential barrier $V_{\mathrm{mw}}(y)$ is created with maximum amplitude in the centre of the trap. This is

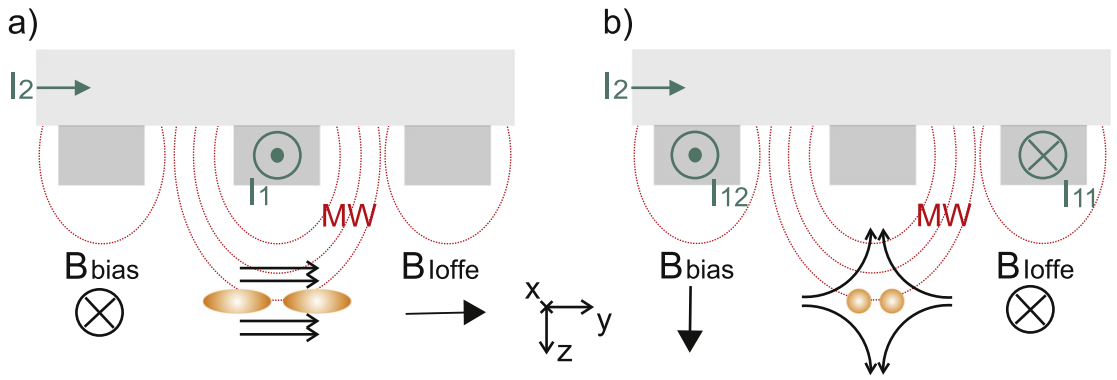

Figure 6. Schematics of the two-layer chip with the main fields for the realization of the MW dressed double well potentials. The currents I_1 (I_{11}, I_{12}) and I_2 flow in dedicated wires in the first and second layer of the chip respectively and contribute together with the Ioffe magnetic field $\mathbf{B}_{\rm Ioffe}$ and a bias field $\mathbf{B}_{\rm bias}$ to the formation of the static magnetic trap where the atoms are kept. The MW field irradiates from the CPW, which is made of three parallel wires as sketched in the figure, see also figure 5. (a) Due to the action of the MW a double well is created along the longitudinal axis of the trap for the two states $|1,\,-1\rangle$ and $|2,\,1\rangle$ when the MW frequency is tuned close to the π-polarization driven transitions as shown in figure 4. (b) An alternative realization of the double well potential with our chip geometry. The splitting in this case takes place along the radial axis of the trap, for MW frequencies close to σ-polarization driven transitions, see later in the text for discussion. In the both cases the direction of the splitting is set by the orientation of the MW field at the position of the atoms.

obtained by exploiting the spatial variation of the Rabi frequency $\Omega^{2,-1}_{1,-1}(\mathbf{r})$ for $F=1$ ($\Omega^{2,1}_{1,1}(\mathbf{r})$ for $F=2$) which is proportional, as explained above, to the projection of the MW field along the direction of the static magnetic field $\mathbf{B}_{\rm mw}(\mathbf{r})\cdot\mathbf{B}(\mathbf{r})/|\mathbf{B}(\mathbf{r})|$. As in the center of the trap $\mathbf{B}_{\rm mw}\,\|\mathbf{B}\,\|\mathbf{y}$, the Rabi frequency and consequently $V_{\rm mw}$ are maximal and decrease moving along the y axis, creating the desired double-well potential. For the other allowed transitions, the Rabi frequency depends instead on the component of the MW field perpendicular to the direction of the static field $\mathbf{B}_{\rm mw}(\mathbf{r})\times\mathbf{B}(\mathbf{r})/|\mathbf{B}(\mathbf{r})|$ and the resulting MW potentials mainly shift the vertical position of the cloud without leading to the formation of a double-well. As the final dressed potential is approximately a sum of the different contributions associated with all the possible MW-induced transitions, we minimize unwanted effects by setting the MW frequency such that $\Delta \ll \mu_B|\mathbf{B}_{\rm Ioffe}|/(2\pi\hbar) \simeq 4$ MHz. In our working configuration the MW is thus blue(red)-detuned with respect to the $|1,\,-1\rangle \rightarrow |2,\,-1\rangle$ transition for the atoms in $F=1$ ($|2,\,1\rangle \rightarrow |1,\,1\rangle$ transition for the atoms in $F=2$) as depicted in figure 4. We stress that the dominant elements which we employ to engineer $V_{\rm mw}(\mathbf{r})$ are: the spatial dependence of the MW field $|\mathbf{B}_{\rm mw}(\mathbf{r})|$, of its polarization and the spatial dependence of the Zeeman shift due to the static field $\mathbf{B}(\mathbf{r})$. The size of the achievable double-well potentials is thus strongly related to the geometry of the CPW and to its distance from the position of the atoms, as well as to the frequencies of the static magnetic trap. Notably, by playing with these parameters, splitting distances much smaller than the wavelength of the radiation employed can be achieved at a suitable distance from the chip.

3.1. Characterization of the MW mode delivered by the chip

The MW field delivered by the CPW is characterized similarly to [20]. We start preparing a cloud of 2×10^6 atoms of ^{87}Rb at a temperature of $T=10\,\mu$K in the hyperfine sublevel $|F,\,m_F\rangle = |1,\,-1\rangle$. We then switch off all the laser beams and confining magnetic fields, letting the atoms expand in a static homogeneous magnetic field $B_{\rm bias}\simeq 3$ G, selectively pointing along the x, y or z axis. During expansion we pulse the MW-field with frequency resonant on the transitions $|1,\,-1\rangle \rightarrow |2,\,m_F=-2,\,-1,\,0\rangle$ and we selectively image the atoms in the $F=2$ hyperfine state, see figure 7 (left). Varying the pulse duration, we can map the Rabi oscillation for the three different polarization components with different orientations of the bias field. The intensity of the MW field $B_{\rm mw}(\mathbf{r})$ and the relative weight of the different polarizations, in particular, are measured. We fit the MW-mode by means of a static field calculation. We can best reproduce the experimental data by considering an asymmetry of $0.16I_{\rm mw}$ in the current distribution of the external grounded wires of the CPW (ideally $I_l = I_r = -I_{\rm mw}/2$ where I_l, I_r, $I_{\rm mw}$ are respectively the currents in the left, right and central wires of the CPW, see also [21]) and by assuming an induced current with amplitude $0.1I_{\rm mw}$ in one of the closest wires to the CPW. One example of the measured Rabi frequency, on the transition $|1,\,-1\rangle \rightarrow |2,\,-1\rangle$ (π polarization) with $\mathbf{B}_{\rm bias}\|\mathbf{y}$, is shown in figure 7 (right) together with the corresponding simulation, for two different distances from the chip surface.

3.2. Realization and characterization of a double-well potential on an atom chip

In order to test the above predictions, we first show experimental results obtained by dressing just one of the two ground states, $|1,\,-1\rangle$. The final potential to the atoms is characterized experimentally by measuring the

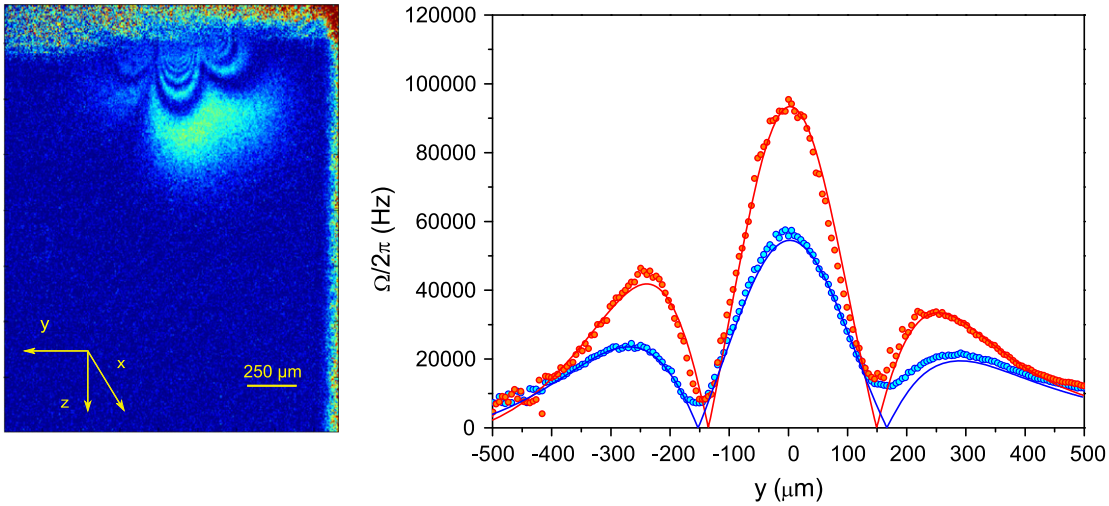

Figure 7. (Left) Atoms imaged in $F = 2$ after a MW-pulse resonant on the $|1, -1\rangle \rightarrow |2, -1\rangle$ transition with power 10 mW and $\mathbf{B} \equiv \mathbf{B}_{\text{bias}} // \mathbf{y}$. The spatial modulation of the Rabi frequency is visible for a fixed duration of the pulse. On the upper side of the figure the shadow cast by the chip is visible. (Right) Points: measured Rabi frequency $\Omega_R(y, z_0)$ with MW-frequency resonant on the $|1, -1\rangle \rightarrow |2, -1\rangle$ and $\mathbf{B}_{\text{bias}} // \mathbf{y}$, here shown for two different distances from the chip $z_0 = 135\,\mu$m (red points) and $z_0 = 185\,\mu$m (blue points). Solid lines: corresponding simulations of the MW-mode.

distance between the potential minima as a function of the MW amplitude delivered by the synthesizer. We prepare a BEC of ~1000 atoms in the state $|1, -1\rangle$. For the experiments described here, the atoms are loaded in a harmonic trap with frequencies $2\pi \times (160, 90, 130)$ Hz and longitudinal axis along the $\mathbf{y}$ direction, at 50 μm distance from the chip surface. We switch on adiabatically the MW with a s-shaped ramp in ~1 s and we measure the density distribution of the atoms after a short time-of-flight (TOF) of few ms. For these measurements, the MW frequency is set to be $\Delta = 500$ kHz blue-detuned with respect to the $|1, -1\rangle \rightarrow |2, -1\rangle$ transition, with a Ioffe field of $B_y = 3.055$ G. Increasing the power of the MW, two separated clouds start to be resolved with increasing separation distance. To correct for an asymmetric atomic population of the two well, mainly due to the underlying asymmetry of the MW field, a constant magnetic gradient of 68 mG cm^{-1} is added. In figure 8(a) we compare our results to the numerical simulations of $V = V_{\text{magn}} + V_{\text{mw}}$ performed by taking into account the actual geometry of the chip wires and MW field, with no free parameters. The agreement with the measurements is good. In figure 8(b) the measurement of the separation distance is shown as a function of the detuning Δ, for a power of 38.9 mW. A non-negligible effect of the MW near-field consists also in pushing the atoms away from the chip due to the presence of a gradient of $|\Omega_{2,-1}(\mathbf{r})|$ along the z axis. Finally we measure the shift of the resonance of the $|1, -1\rangle \rightarrow |2, 1\rangle$ transition for increasing power of the MW field, which we compare to the calculated energy shift induced by the dressing on the coupled levels, figure 8(c). The transition is driven by electro-magnetic pulses of a MW field, 500 kHz blue detuned from the $|2, 0\rangle$ level, and an additional RF field with power low enough not to introduce additional dressing. The agreement with theory is generally good for relatively small splitting distances $d \lesssim 50\,\mu$m. The residual disagreement is to be attributed to the simple modelling of the MW-mode (we estimate local deviations up to 20%, whose effect becomes more important for higher MW powers) and, to a lower extent, of the actual chip trap. This allows us to extrapolate from the simulations, in this range, the functional dependence of double-well barrier height on the splitting distance, which is only smoothly affected by the precise detuning $\Delta_{1,-1}$ chosen, being predominantly set by the magnetic trap frequencies and by the MW-field mode. For our experimental case, we find that to completely split a condensate with chemical potential $\mu/(2\pi\hbar) \sim 100$ Hz, a separation $\gtrsim 30\,\mu$m should be achieved. This rather large separation is due to the smooth variation of $\mathbf{B}_{\text{mw}}$ over the size of the cloud and to the low trapping frequency along the splitting axis, which coincides with the longitudinal axis of the trap.

4. Realization of state-selective potentials on a chip

In the previous section, we have shown that we can use a chip-delivered MW-near field to create a double-well potential, alternatively to the so far employed radio-frequency fields [23]. Moreover a key feature of MW-generated dressed potentials with respect to radio-frequency ones relies on the possibility of independently addressing the internal states used in the beam splitter proposal. The RF field will indeed couple to both the states, limiting the possibilities of independently engineering the wavefunctions of the atoms in the two states.

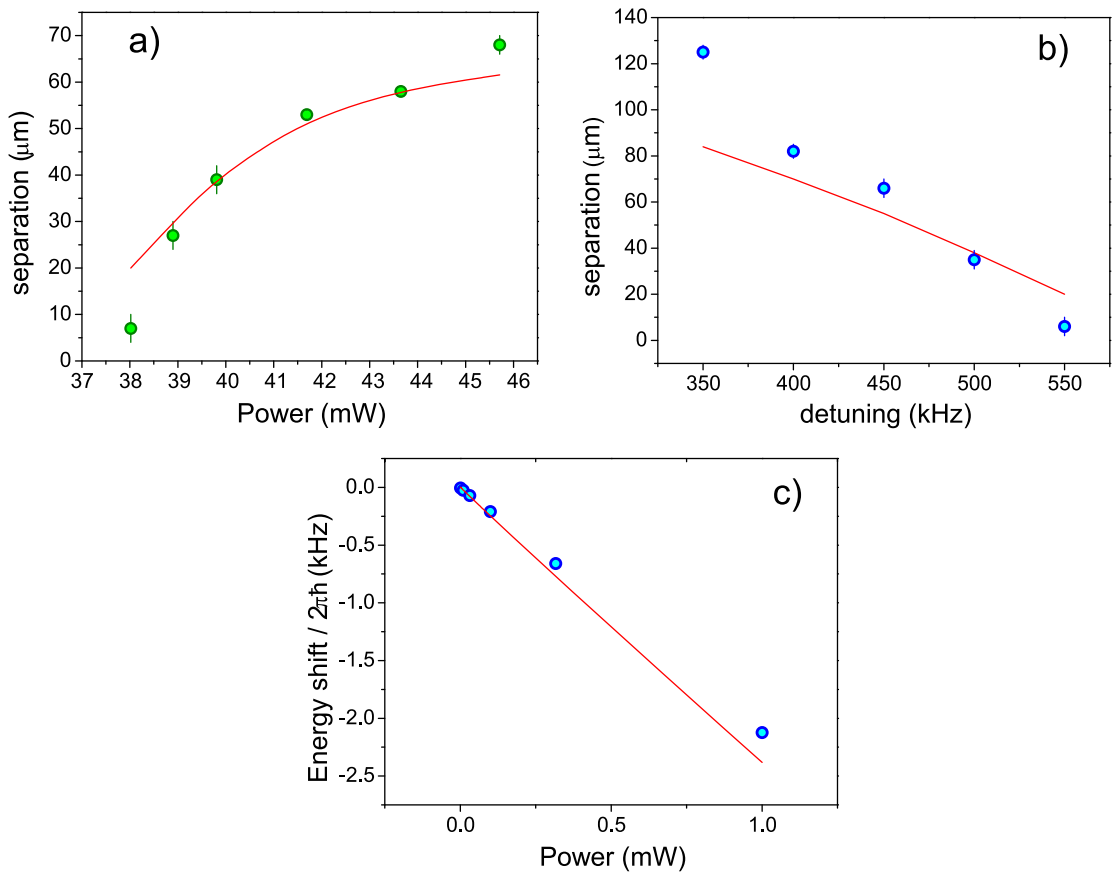

Figure 8. Dressing of $F = 1$ state. (a) Measured cloud separation as a function of the power delivered by the synthesizer with $\Delta = 500$ kHz. Solid line represents the simulations without free parameters. (b) Measured cloud separation as a function of the detuning Δ for $P_{\mathrm{mw}} = 39$ mW with corresponding simulations. (c) Energy shift of the transition $|F = 1,\ m_F = -1\rangle \rightarrow |F = 2,\ m_F = 1$ as a function of the power delivered by the synthesizer for $\Delta = 500$ kHz together with simulations.

As discussed above, the overlap between the wavefunctions plays an important role in determining the feasibility and fidelity of the beam splitter operation and it is thus a crucial parameter to be optimized. The MW field, notably, allows to create state-selective potentials, which can also be independently tuned once two different frequencies are provided.

In order to test this, we dress the atoms by superimposing on the CPW two MW-frequencies delivered by the same synthesizer, which can be independently tuned. In particular we add to the dressing on the $|1,\ -1\rangle \rightarrow |2,\ -1\rangle$ transition, which affects mainly the atoms in $F = 1$, a second frequency close to the $|1,\ 1\rangle \rightarrow |2,\ 1\rangle$ transition for the dressing of the atoms in $F = 2$, as shown in the level scheme of figure 4. Note that due to the Zeeman splitting following the presence of a bias field of ~3.055 G, the two frequencies are far enough (~9.2 MHz) not to give rise to cross interference terms.

We prepare a BEC alternatively in the state $|1,\ -1\rangle$ or $|2,\ 1\rangle$ and we ramp up the two-tone dressing adiabatically. In figure 9 we report the measurements at short TOF of the splitting distance when a double well is formed, with detuning $\Delta_1 = -\Delta_2 = 52$ kHz and power $P_{\mathrm{mw1}} = P_{\mathrm{mw2}}$. A clear double well forms in the $F = 2$ state at lower powers than in $F = 1$. This difference is due to the presence, in the dressed potential of the $F = 1$ state, of an additional repulsive component on the σ^--induced transition $V_{2,-2}$ which shifts the atoms along the z axis to lower values of the MW potential $V_{\mathrm{mw},1}(\mathbf{r})$. The magnetic gradient which is used to symmetrize the atomic distribution within the two wells is optimized to 57 mG cm^{-1} for the atoms in $F = 2$. As shown in figure 9 (left) a working configuration can be easily found in which the atoms in $F = 2$ are well split into a double-well while the atoms in $F = 1$ are still trapped within a single well. Dressing of $F = 1$ state can be further independently manipulated in order to adjust the shape and position of the initial cloud.

4.1. Transfer and spectra

In order to study the transfer of the atoms from $|1,\ -1\rangle$ to $|2,\ 1\rangle$, when different external potentials are applied to the two states, we drive a 2 photon transition, as written in section 3.2, while applying different two-tone dressings. We perform, in particular, a weak pulse of duration 300 ms and measure the relative population of the transferred atoms $P_2 = N_2/(N_1 + N_2)$, where N_1, N_2 are imaged in TOF by means of a double-state detection

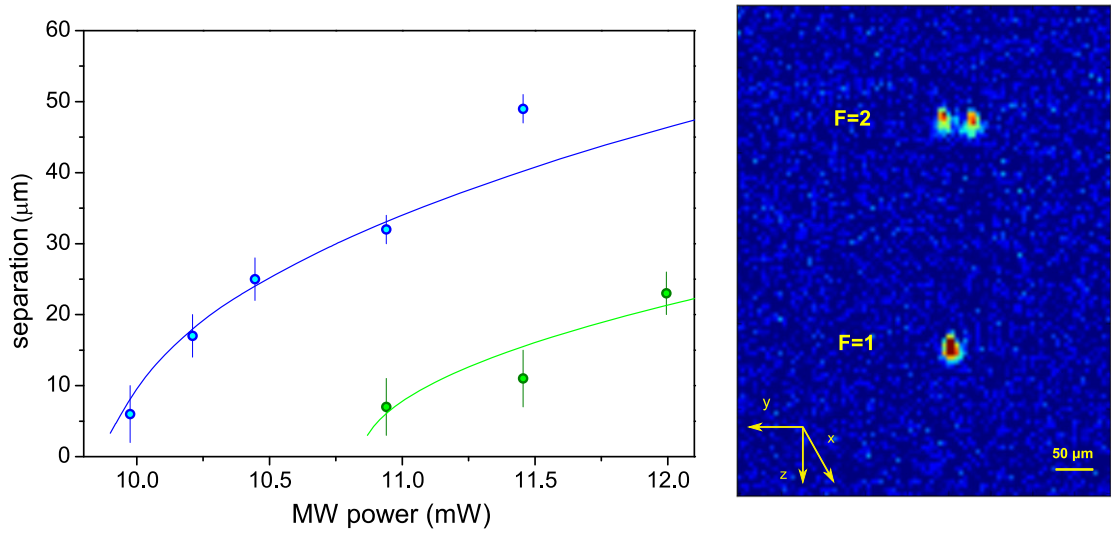

Figure 9. (Left) Simultaneous two-tone dressing of $F=1$ and $F=2$ with $\Delta_1 = -\Delta_2 = 52$ kHz and equal power delivered by the synthesizer in the two tones. The atoms are all either in $F=1$ or in $F=2$, and they are detected at the same TOF. The solid lines are fits to the data obtained by using the numerical simulations of the fields with the mw amplitude as a free parameter. (Right) Double state detection of the atoms in $F=1$ and $F=2$. Here the atoms are prepared in the two states and simultaneously dressed by a two-frequency MW radiation. Vertical separation is due to the different time at which the imaging is performed for the two states (15 and 17 ms TOF respectively).

technique. Scanning the frequency of the RF photons, we can get the spectrum of the final potential in $F=2$. We repeat the measurements for different powers of the MW-dressing which correspond to different realizations of the two external potentials. In figure 10 we show the experimental results, for $\Delta_1 = -\Delta_2 = 52$ kHz and $P_{\mathrm{mw}-1} = P_{\mathrm{mw}-2} = P_{\mathrm{mw}} = 10,\ 10.5,\ 11,\ 11.5$ mW, which are fitted with a simple 1D model. We calculate the eigenstates $\psi_i(y)$ and energy spectrum ξ_i of an ideal double-well potential $V(y) = \frac{V_0}{(d/2)^4}(y^2 - (\frac{d}{2})^2)^2$ with separation between the wells d and barrier height V_0 as adjustable parameters. The wavefunction of the atoms in $F=1$, which we assume to be all in the ground state of the harmonic potential, is simply written as $\varphi(y) = \frac{1}{\sqrt{2\pi}\sigma}\mathrm{e}^{-(y-y_0)^2/(2\sigma^2)}$. The coupling strength is given by $\Omega(\nu) = A\sum_i \frac{C_i}{1+(\nu-\nu_i-\nu_c)^2/w^2}$ with $C_i = |\int \psi_i^*(y)\varphi(y)\mathrm{d}y|$ and $\nu_i = \xi_i/(2\pi\hbar)$, where w is the spectral width of the pulse and ν_c an offset frequency. The parameters d, y_0 and σ have been experimentally determined. This simple model does not account for interactions between the atoms, however it can still provide an understanding of the spectra without the need of too involved calculations. In particular, it reproduces quite well the measurements at higher values of the power $P_{\mathrm{mw}} = 11.5,\ 11$ mW. In this case the atoms in $F=1$ are mainly pushed to one side along the y axis by the dressed potential $V_{\mathrm{mw}-1}$ and thus better couple to just one of the two double-wells (see insets of figure 10). For lower P_{mw} the atoms are less displaced from the center of the unperturbed trap, and the initial wavefunction $\varphi(y)$ starts to be more symmetrically distributed over the two wells. The worse agreement with the simple model, which is observed for these powers of the dressing, can be explained with the existence of asymmetries on the double-well potential which are not caught by our ideal representation of the potential $V(y)$. We can estimate this asymmetry to be $15 - 20\%$ in the range of MW power considered here. This measurement has been performed by fast transferring the atoms to the top of the potential barrier of the double well. The cloud then fragments into two pieces following a complete oscillation in each of the two wells, from which we can derive the trapping frequencies. By comparison with the simple theory we can, however, identify the eigenstates of the external potential which the transfer occupies. We can also derive an estimation of the barrier height, which is plotted, for comparison, together with the simulations of the potential in figure 11.

Finally we note that the dressing on the $|1,\ -1\rangle$ state is necessary to maintain a finite wavefunction overlap between the atoms in $F=1$ and $F=2$ along the z axis. Without this correction to the potential of the $F=1$ atoms, the two clouds would be displaced vertically by a distance of 15 μm for our experimental parameters, which is larger than their radial extension. A fine tuning of the potentials $V_{\mathrm{mw}-1}$ and $V_{\mathrm{mw}-2}$ is shown in figure 11 where transfer spectra have been measured for different detuning Δ_1. A difference in the vertical position within the two clouds d_z leads to the appearance of additional sidebands corresponding to the vertical trapping frequency with coupling elements $\Omega_{F=1,n=1\to F=2,n'=2} = \langle F=2,\ n'=2|\Omega_{2ph}\mathrm{e}^{\frac{\mathrm{i}d_z\hat{p}_z}{\hbar}}|F=1,\ n=1\rangle$, where $\hat{p}_z$ is the momentum transfer along z axis. The best wavefunction overlap for the two clouds along the vertical direction is found for $|\Delta_1| > |\Delta_2|$ with equal MW-power $P_{\mathrm{mw}-1} = P_{\mathrm{mw}-2}$.

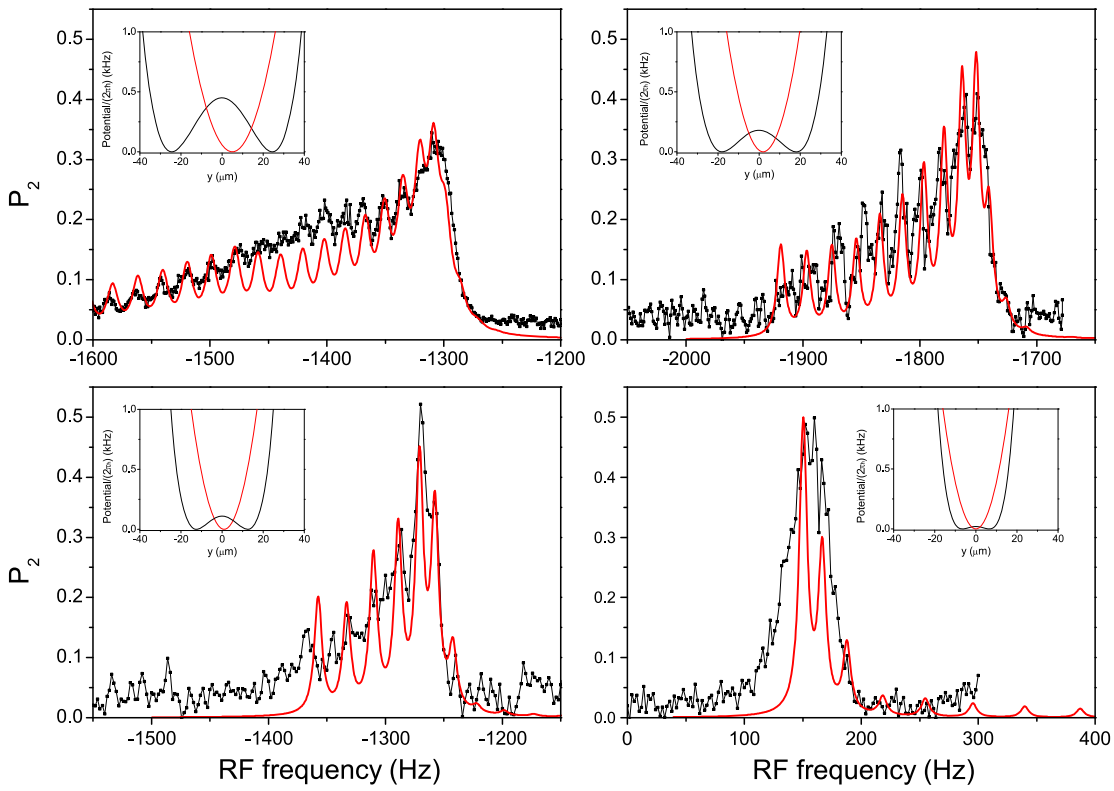

Figure 10. Relative number of transferred atoms P_2 from $|1, -1\rangle$ to $|2, 1\rangle$ for different powers of the dressing field $P_{mw} = 11.5, 11, 10.5, 10$ mW, corresponding to different depths (and minima separations) of the double-well potential. These measurements are the average over (20, 10, 5, 10) acquisitions respectively. Red solid lines are fits with a single-particle 1D theory (see main text for details). Insets show the potentials in $F = 1$ (red solid line) and $F = 2$ (black solid line) which correspond to the fits (see text).

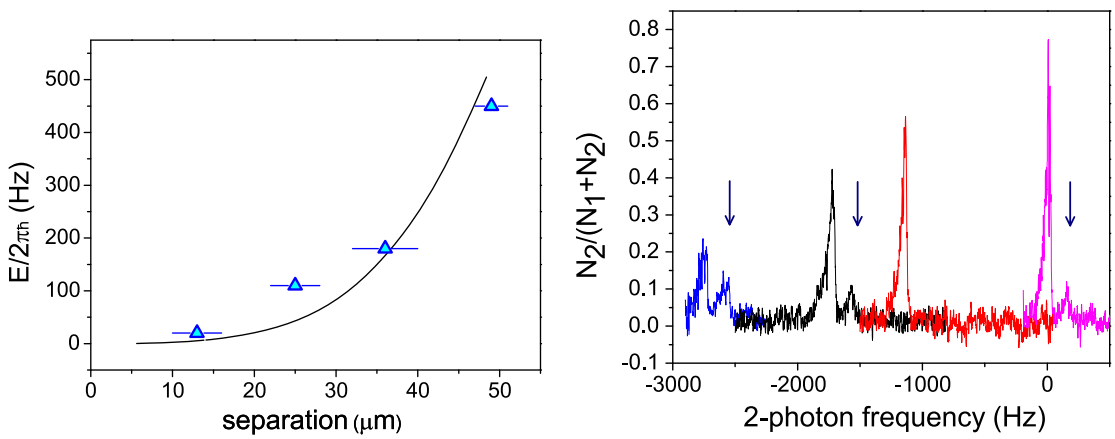

Figure 11. (Left) Calculated energy height of the double-well barrier E as a function of the separation between the minima of the potential. For comparison we plot the measurements of E, blue points, obtained by means of a simple fit of the spectra for atoms in $F = 2$. Note that the simulated $E(d)$ does not vary significantly with the exact frequency of the detuning and with the internal state. (Right) Relative number of transferred atoms as a function of the 2-photon frequency for different dressing of the $F = 1$ state only. We vary in particular the detuning (from left to right): $|\Delta_1| = (\Delta_2 - 9), (\Delta_2 - 3), (\Delta_2 + 3), (\Delta_2 + 10)$ kHz with equal power delivered in the two tones. Sidebands generated by the cloud displacement are visible at frequencies compatible with the trapping along the vertical axis.

Finally, by tuning the frequency of the pulse, for a π pulse duration $\tau \gg 2\pi/\omega_{ho}$, we can thus address different single external states of the double-well potential in $F = 2$. For a given power, the transfer to the ground state, as shown by the spectra, turns out to be significantly less consistent with respect to the high-energy states closer to the barrier height due to bad wavefunction overlap. This problem can be, to some extent, circumvented as the wavefunction of the atoms before the transfer can be independently modified and the wavefunction overlap along the y axis further optimized.

On the other extreme, fast transfers $\tau \ll 2\pi/\omega_y$ lead to a rather different scenario with the coherent occupation of several vibrational states of the double-well in $F = 2$. Once transferred the atoms find themselves out of equilibrium with respect to the new external potential: the single BEC thus splits in two fragments which follow their own dynamics rolling down the potential hill and coming back after an oscillation period to recombine. This configuration presents some similarities with the in-trap splitting of a BEC by means of optical Bragg diffraction [24], and it could be considered for a matterwave analog of a white light interferometer.

5. Discussion and conclusions

In the previous paragraphs we have demonstrated the possibility to realize double-well potentials, selectively on the atomic internal state, by the use of MW fields delivered by the chip structures. Furthermore, by applying appropriate Rabi pulses we can transfer the atoms selectively to one external state of the double-well potential. However our peculiar chip device shows some limitations due to the large separation ($\gtrsim 30\ \mu$m) between the potential minima which is needed to achieve a barrier height safely bigger than the BECs chemical potentials. Given the relatively shallow radial frequencies, we experience a limit in the possibility of adjusting the potential of the state $|1\rangle$ due to the need of maintaining a sufficient wavefunction overlap along the vertical direction. As a result, the maximum overlap among the wavefunctions in $|1\rangle$ and $|2\rangle$ is below 1%. This requires long transfer times and non-trivial engineering of the Rabi pulses in order to achieve an useful transfer efficiency. To obtain a separated double well with smaller splitting distances of a few microns, the CPW transverse dimension could be reduced by an order of magnitude (as in [21]) or the trapping frequency could be increased. In this second case, a CPW with the same dimensions as ours can be exploited to realize a static magnetic trap with weak axis parallel to the axis of the CPW, i.e. $\mathbf{B}_{\mathrm{Ioffe}} \| \mathbf{x}$ see figure 6. A double-well is formed along the radial direction of the trap, y direction in the figure, by properly blue-detuning the MW-field to the σ-induced transition ($\Delta m_F = -1$) for the atoms in $F = 1, 2$. This configuration can be used to obtain an experimental implementation of the simulations presented in the second paragraph. However, in the current version of the experiment we are limited to the unique realization described here, as the side wires of the CPW cannot be independently controlled (they are grounded together at the chip). Conversely, a new version of our experiment, which is now under construction, will meet these requirements. We finally notice that the splitting direction is set by the orientation of the MW field at the position of the atoms, thus, in order to modify it, a different design of the CPW would be required.

To conclude, we have proposed a novel beam splitter technique for BECs which does not require a dynamical deformation of the trapping potential. This allows the preparation of an initial clean coherent state in a double-well potential without the formation of spurious, unwanted, excitations. We have numerically shown that the ground state of a double-well potential can be coherently and rapidly populated with excellent fidelity and efficiency without the use of optimal control techniques, with realistic simulation numbers. By studying an experimental case, we present the first realization of a MW-dressed double-well potential selectively on one internal state of ^{87}Rb and we prove at the same time independent control on the potentials of the two different internal states. We have also characterized the transfer procedure and the addressing of different vibrational states in the double-well. This work shows that to obtain a good transfer efficiency and fidelity in reasonable transfer times, the wavefunction overlap between the initial and final states should be optimized. This is achievable with current state-of-the-art experiments, promoting our technique as a very promising tool in the field of atom interferometry with BECs, e.g. by opening the possibility to monitor the dynamical formation of non-trivial entangled states with metrological gain. We finally note that this system constitutes a potential realization of the long discussed spin-boson model [25], which would allow the study of decoherence processes in a controlled environment [26].

Acknowledgments

We would like to thank Philipp Treutlein, Andrea Trombettoni, Luca Pezzé and Wilfried Maineult for fruitful discussions. This work was supported by the French National Research Agency within the project CATS ANR-09-NANO-039 and by the European Metrology Research Program (EMRP) under the project IND14. The EMRP is jointly funded by the EMRP participating countries within EURAMET and the European Union.

References

[1] Cronin A D, Schmiedmayer J and Pritchard D E 2009 *Rev. Mod. Phys.* **81** 1051
[2] Esteve J, Gross C, Weller A, Giovanazzi S and Oberthaler M K 2008 *Nature* **455** 1216
[3] Gross C, Zibold T, Nicklas E, Estve J and Oberthaler M K 2010 *Nature* **464** 1165
[4] Reidel M F, Bohi P, Li Y, Haensch T W, Sinatra A and Treutlein P 2010 *Nature* **464** 1170

[5] Lewenstein M and You L 1996 *Phys. Rev. Lett.* **77** 3489
[6] Shin Y, Saba M, Pasquini T A, Ketterle W, Pritchard D E and Leanhardt A E 2004 *Phys. Rev. Lett.* **92** 050405
[7] Schumm T, Hofferberth S, Anderson L M, Wildermuth S, Groth S, Bar-Joeseph I, Schmiedmayer J and Kruger P 2005 *Nat. Phys.* **1** 57
[8] Berrada T, van Frank S, Bucker R, Schumm T, Schaff J-F and Schmiedmayer J 2013 *Nat. Commun.* **4** 2077
[9] Menotti C, Anglin J R, Cirac J I and Zoller P 2001 *Phys. Rev.* A **63** 023601
[10] Streltsov A I, Alon O E and Cederbaum L C 2007 *Phys. Rev. Lett.* **99** 030402
[11] Faust D K and Reinhardt W P 2010 *Phys. Rev. Lett.* **105** 240404
[12] Huang Y P and Moore M G 2006 *Phys. Rev.* A **73** 023606
[13] Piazza F, Pezzé L and Smerzi A 2008 *Phys. Rev.* A **78** 051601
[14] Zibold T, Nicklas E, Gross C and Oberthaler M K 2010 *Phys. Rev. Lett.* **105** 204101
[15] Boukobza E, Chuchem M, Cohen D and Vardi A 2009 *Phys. Rev. Lett.* **102** 180403
[16] Beaufils Q, Tackmann G, Wang X, Pelle B, Pelisson S, Wolf P and Pereira dos Santos F 2011 *Phys. Rev. Lett.* **106** 213002
[17] Zhang W and Walls D F 1994 *Phys. Rev.* A **49** 3799
[18] Wang H 2007 *J. Comput. Appl. Math.* **205** 88
[19] Nistazakis H E, Rapti Z, Frantzeskakis D J, Kevrekidis P G, Solano P and Trombettoni A 2008 *Phys. Rev.* A **78** 023635
[20] Bohi P, Riedel M F, Haensch T W and Treutlein P 2010 *Appl. Phys. Lett.* **97** 051101
[21] Bohi P, Riedel M F, Hoffrogge J, Reichel J, Haensch T W and Treutlein P 2009 *Nat. Phys.* **5** 592
[22] Maineult W, Deutsch C, Gibble K, Reichel J and Rosenbusch P 2012 *Phys. Rev. Lett.* **109** 020407
[23] Hofferberth S, Lesanovsky I, Fischer B, Verdu J and Schmiedmayer J 2006 *Nat. Phys.* **2** 710
[24] Horikoshi M and Nakagawa K 2007 *Phys. Rev. Lett.* **99** 180401
[25] Leggett A J, Chakravarty S, Dorsey A T, Fisher M P A, Garg A and Zwerger W 1987 *Rev. Mod. Phys.* **59** 1
[26] Scelle R, Rentrop T, Trautmann A, Schuster T and Oberthaler M K 2013 *Phys. Rev. Lett.* **111** 070401